Computational Materials Science 49 (2010) 582–587

Contents lists available at ScienceDirect

Computational Materials Science

journal homepage: www.elsevier.com/locate/commatsci

Onset of failure in argon by the effect of a shockwave: A molecular dynamics study

Claudia Loyola *, Sergio Davis [1], Joaquín Peralta, Gonzalo Gutiérrez

Group of NanoMaterials, Departamento de Física, Facultad de Ciencias, Universidad de Chile, Casilla 653, Santiago, Chile

ARTICLE INFO

Article history:
Received 29 March 2010
Received in revised form 13 May 2010
Accepted 27 May 2010
Available online 26 June 2010

Keywords:
Shockwave
Molecular dynamics
Non-equilibrium

ABSTRACT

Molecular dynamic simulations of shockwaves in solid argon were performed. The simulation cell contains 51,840 atoms at 5 K interacting by means of a pairwise potential. The shockwave itself was introduced explicitly in the simulation by a piston hitting the sample from one side of the simulation box, at speeds ranging from 1.2 to 1.3 times the speed of sound in solid argon at the chosen density. In order to characterize the sample in terms of both structural and dynamic properties, we determine the density and temperature profiles according the advance of the shockwave, evaluating, for different slabs, the pair–distribution function, coordination number as well as performing a common neighbor analysis for the atoms. Our simulations reproduce the experimental Hugoniot curve and show how the material is break due to rarefaction waves. The picture that emerges is that when the shockwave starts, a local melting is produced in a region of the sample. Then, as the shockwave travels through the sample, a high density disordered phase is identified. When the piston stops, a rarefaction wave develops, producing a large tensile stress, which finally causes the failure of the sample.

1. Introduction

Among the different physical properties of materials, the knowledge of the mechanical behavior is fundamental for practical applications, but is also important from a more basic point of view [1]. As a matter of fact, in the study of materials at extreme conditions, e.g. at high temperature and pressure, there are a number of phenomena which in the normal, equilibrium conditions, are not present and/or are almost impossible to foresee, and for which there is a poor understanding. For example, the dynamic failure due to a tensile strength, despite the intensive research, so far cannot be precisely determined by theoretical means and there is no clear explanation relating the macroscopic behavior to the atomic level [2–4].

One of the methods used to study the response of materials to extreme conditions is the shockwave experiment. Typically, in such experiments the sample reaches a pressure up to 300 GPa and peak temperatures that melt locally the sample [5]. Several approaches has been used to study shockwaves in solid, ranging from hydrodynamics approximation [6,7] to atomistic simulation. In particular, molecular dynamics (MD) simulation has been successfully employed, demonstrating that the microscopic mechanism of their propagation is intrinsically more complex than in a fluid, because the plastic flow is governed by the creation and motion of defects, and not only by viscous dissipation [8–14].

In this paper we report a MD study of the failure of a solid argon due to the passage of a shockwave. We consider here argon because it represent a generic solid for which a wide range of properties have been studied, both from the experimental and theoretical point of view. For instance, Stishov et al. [15] obtained the melting curve up to 322 K and 15,835 kg/cm^2. After that, Ross et al. [16] compared the static high pressure and shockwave equation of state, and concluded that solid argon may provide a useful static pressure standard up to about 34 Mbar. This is important because most diamond anvil experiments are performed within an argon atmosphere, and a detailed knowledge of the equation of state is crucial in order to ensure the correct interpretation of the measurements [17].

We give a detailed atomistic description of the process, similar to the spallation phenomena, stressing the structural and dynamical changes that take place, including the creation of defects and void growth, which finally results in the mechanical failure of the sample.

The organization of this paper is as follows. In Section 2 we describe the computational procedure and validation of the model. In Section 3 we show the effects of the shockwave propagation on the material. In Section 4 we summarize the results.

2. Computational procedure

The MD was performed in the microcanonical ensemble, using a tetragonal simulation cell containing 51,840 argon atoms, initially in a fcc structure with a density of 1.42 g/cm^3, with box lengths of

* Corresponding author.
E-mail addresses: claudial.81@gmail.com (C. Loyola), sergdavis@gmail.com (S. Davis), jperaltac@gmail.com (J. Peralta), gonzalo@fisica.ciencias.uchile.cl (G. Gutiérrez).
URLs: http://www.gnm.cl (C. Loyola), http://fisica.ciencias.uchile.cl/~gonzalo (G. Gutiérrez).
[1] Address: Royal Institute of Technology (KTH), Stockholm, Sweden.

0927-0256/$ - see front matter © 2010 Elsevier B.V. All rights reserved.
doi:10.1016/j.commatsci.2010.05.052

$x = y = 68.4764$ Å and $z = 513.573$ Å [18]. The interatomic interaction is represented by an empirical two-body force fields of the Buckingham type,

$$\phi(r) = B_1 \exp\left(-\frac{r}{r_0}\right) - \frac{B_2}{r^6},$$

where $B_1 = 6127.097$ eV, $r_0 = 0.285$ Å and $B_2 = 61.5497$ eV Å^6. This potential, due to Ross [19], has been developed for argon at extreme conditions, and successfully used in previous shockwave simulations [5].

The sample was thermalized to 5 K during $5000\Delta t$, with $\Delta t = 1$ fs, and then was relaxed during $5000\Delta t$. The piston that compress the sample consisted of 728 atoms (three atomic layers), located at one extreme of the box, along the z direction. On the other extreme of the box the first three layers play the role of a fixed wall. Periodic boundary conditions exist in the x and y directions.

The shockwave is produced by giving the piston a fixed velocity in the z axis during 4000 steps, and then stopped. In this way, a shockwave front travels across the sample, and also a rarefaction wave is developed in the opposite direction. In order to check the reliability of our simulation, we performed several runs with different piston velocities U_p, which produce different shockwave velocities U_s. We repeated the process using different number of particles and box lengths, confirming the same behavior. In this way, we obtained the Hugoniot curve [20,19], displayed in Fig. 1, which presents a good agreement with respect to the experimental data. The Hugoniot curve is a relationship between the parameters of states reached by shock compression, is used to construct the equation of state of the material. The conservation laws for shockwave front is described by the Rankine–Hugoniot equations,

$$V = V_0\left(1 - \frac{U_p}{U_s}\right), \tag{1}$$

$$P = P_0 + \rho_0 U_p U_s, \tag{2}$$

and

$$E = \frac{1}{2}(P - P_0)(V_0 - V). \tag{3}$$

After checking the validity of our model, we perform the actual analysis about the effect of the shockwave in the sample. In this case, to produce the shockwave we assign to the piston a velocity $U_p = 0.5$ km/s, generating a shockwave front with a maximum velocity of $U_s = 1.9$ km/s, both in the z direction. Of course, because we stop the piston after a while, the velocity of the shockwave

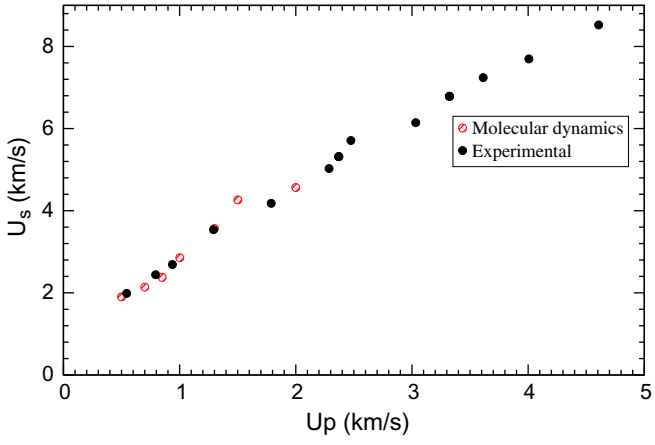

Fig. 1. Piston velocity versus shockwave velocity: experimental and simulation data.

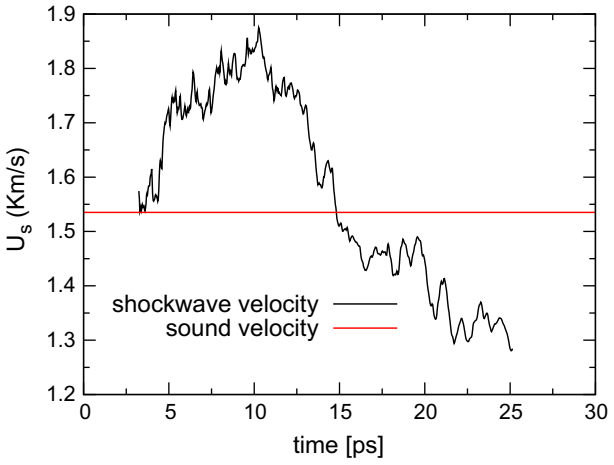

Fig. 2. The instantaneous velocity of the shockwave front in function of time.

front decreases in time, which is shown in Fig. 2. In fact, after some time the shockwave front gets a velocity below the speed of sound in argon (1535 m/s ≈ 1.5 km/s) [21], and is not a shockwave any longer [9,22], becoming a soundwave.

When the piston stops, a rarefaction wave is developed, causing the failure of the sample at the end. In fact, in Fig. 3 we display three stages of this process, coloring atoms by their temperature: (a) the shockwave advances just before the piston stopped. Note the difference between the high density shockwave front at one side (right) and the undisturbed material in the other side (left); (b) the shockwave front is advancing across the sample; (c) finally, void growth can be seen at the right side after the passage of the shockwave.

3. Results

The process just described is studied in detail by using several diagnostics, in which the piston was not considered. Firstly, we quantify the variation of density $\rho(z)$, temperature $T(z)$ and stress $\sigma(z)$, while the shockwave advances across the box. Then we perform a common neighbor analysis (CNA) [23] and the coordination number along the box as a function of time. Finally, around the zone where the material fails we evaluate the pair–distribution function at different times, and show snapshots according an order parameter built from the common neighbor analysis, as well as according the coordination number.

The pair–distribution function $g(r)$ is defined in such a way that, sitting on one atom, the probability of finding another one atom in a spherical shell between r and $r + \Delta r$ is $\langle n(r, r + \Delta r)\rangle = \rho 4\pi r^2 g(r)\Delta r$, where $\rho = N/V$ is the density. The coordination number cn can be obtained by integration around the first peak in the pair–distribution function $g(r)$

$$cn(R) = 4\pi\rho \int_0^R g(r) r^2\, dr, \tag{4}$$

where R is a cutoff, usually chosen as the position of the minimum after the first peak of $g(r)$.

The CNA is a method for analyzing structures by a decomposition of the pair–distribution function according to the local environment of the bonded pairs. The CNA is represented by diagrams that are classified by a set of four indexes. The first index i has values 1 or 2 indicating that a pair of atoms α and β are nearest neighbors ($i = 1$) or not ($i = 2$); the second index j, indicates the number of neighbors common to both atoms (α and β); the third index k is the number of bonds between the common neighbors;

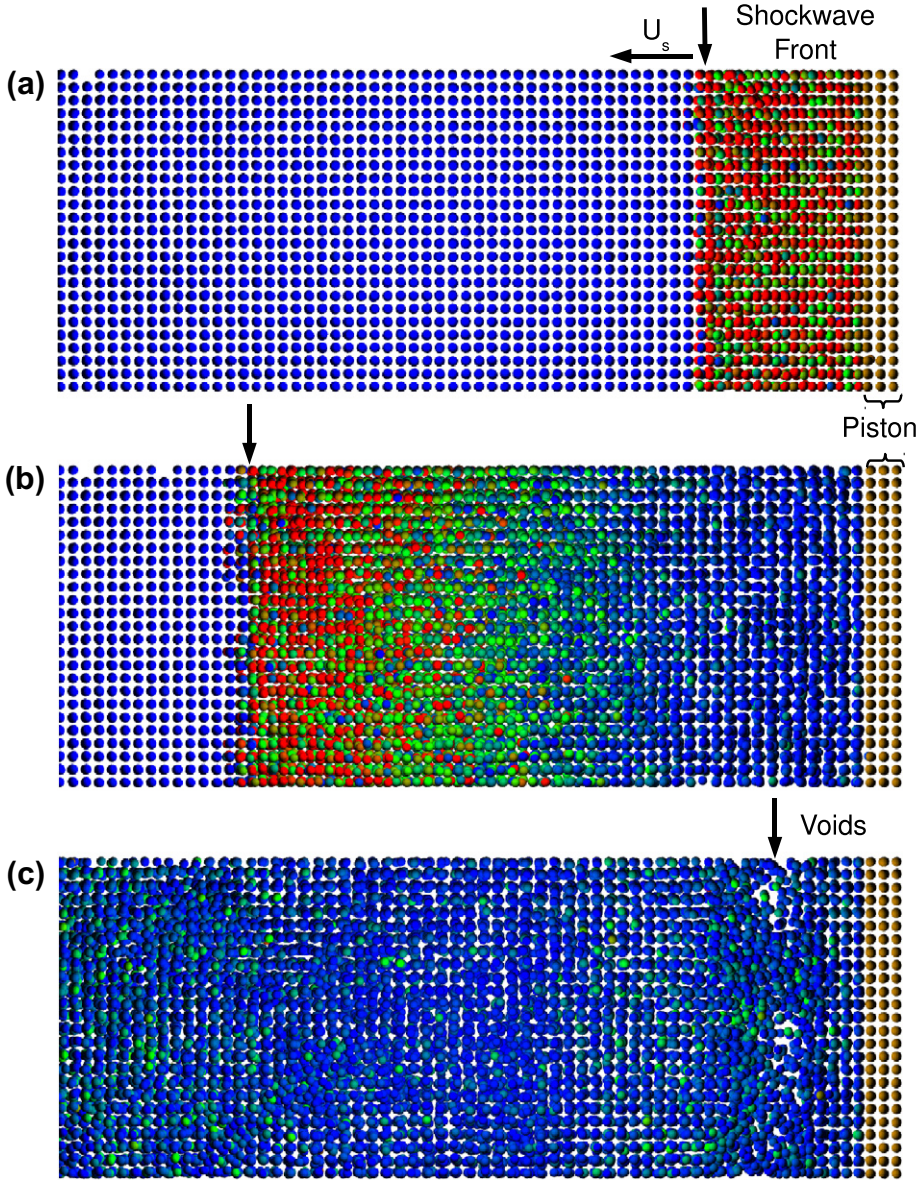

Fig. 3. Snapshots of the shockwave passing across the sample, from right to left, at three different times. Color indicate temperature, from low temperature (blue) to high temperature (red). (a) Top panel show the sample at $t = 3$ ps just before the piston stopped, (b) at $t = 9$ ps the shockwave crossing the sample, (c) at $t = 21$ ps, voids begin to form at the region indicated by the arrow. (For interpretation of the references to color in this figure legend, the reader is referred to the web version of this article.)

and the last index l is the length of the longest continuous chain formed by those k bonds. From the common neighbor analysis, we built an order parameter as follows: in the ideal fcc structure each atom has 12 neighbors, thus participating in 24 pairs 1-4-2-1. Then we can assign a number between zero (perfect fcc) and one (disorder) to each atom, corresponding to the fraction of 1-4-2-1 (fcc-like) pairs. This order parameter is averaged over bins in the z direction in the same way as the other properties.

3.1. Shockwave crossing the material

Figs. 4–6 show the change of the density, temperature and stress along the z direction of the sample as a function of time. These values were obtained by dividing the simulation box in slabs, corresponding to 45 bins along the z direction (each bin containing approximately 1152 atoms). Time is given in picoseconds in all figures.

It can be seen that the density, Fig. 4, increases at the beginning, reaching a density of 1.41 times its initial value (approximately 2.0 g/cm^3). This peak in density clearly shows the width of the shockwave front, and its position shifts to the left as the shockwave passes across the sample. Of course, because we are dealing with a supersonic wave, the density ahead of the shockwave is not affected. Note that the amplitude of the peak decreases in time and its width broadens, due to the energy loss of the shockwave. At the same time, a rarefaction wave develops [24], which can be seen clearly at $t = 12$ ps, and causes the density behind the shockwave front to decrease to a level below the initial value. At the end, this rarefaction wave is responsible for the failure of the material in the region between 453 Å and 484 Å. This picture is consistent with the temperature and stress behavior, which shows, at the beginning, a highest peak about 500 K and 900 MPa, respectively. Note that the temperature decreases monotonically on the shockwave front. Finally, the sample temperature is higher than the one in the initial state.

Also, after the passage of the shockwave the sample has lost its long range order, changing from the initial fcc order to a structure different from that. This conclusion is reached by means of the

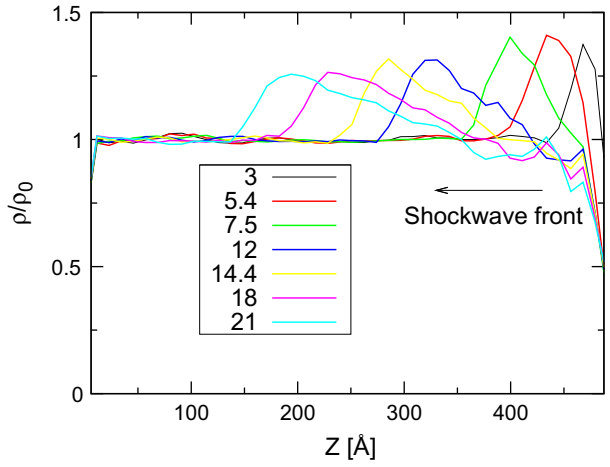

Fig. 4. Density profile $\rho(z)$ along the z direction, at different times (see inset in ps). ρ_0 is the initial density. The shockwave front is passing across the sample from right to left, as the arrow indicates.

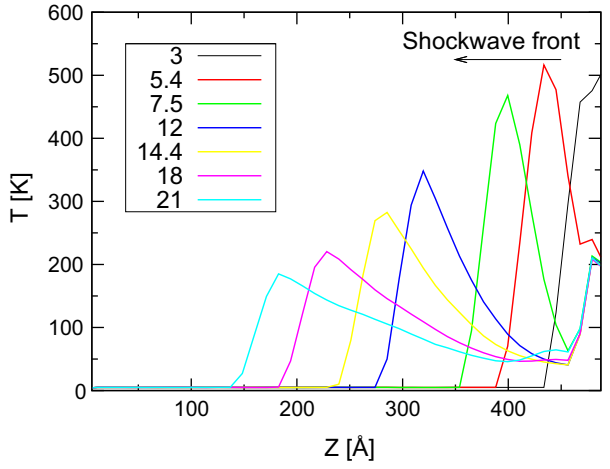

Fig. 5. Temperature profile $T(z)$ along the z direction, at different times (see inset in ps). The shockwave front is passing across the sample from right to left, as the arrow indicates.

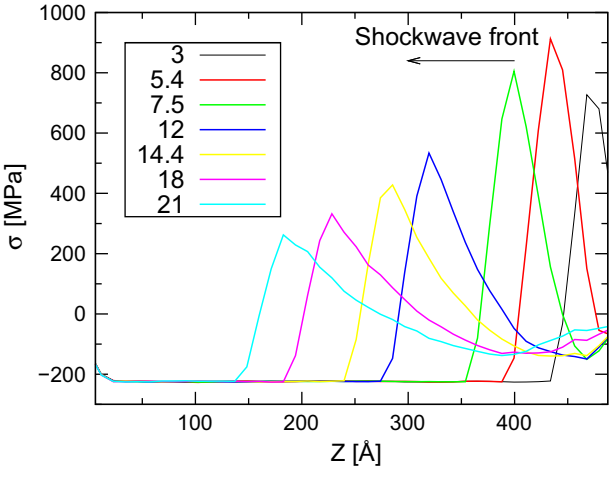

Fig. 6. Stress profile $\sigma(z)$ along the z direction, at different times (see inset in ps). The shockwave front is passing across the sample from right to left, as the arrow indicates.

common neighbor analysis and the coordination number. Fig. 7 displays the CNA order parameter for different times. We can see

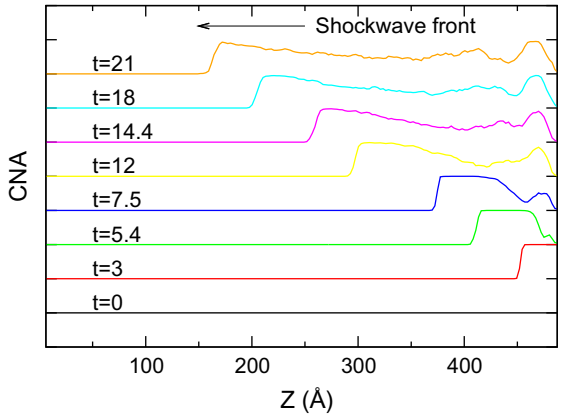

Fig. 7. CNA order parameter along the z direction, at different times (see inset in ps). At the initial time $t = 0$, CNA order parameter is zero, which means a fcc lattice. Values greater or lesser that zero means an order (or "disorder") different from fcc. Curves at different times have been shifted for clarity. In the figure, the shockwave front is passing across the sample from right to left, as the arrow indicates.

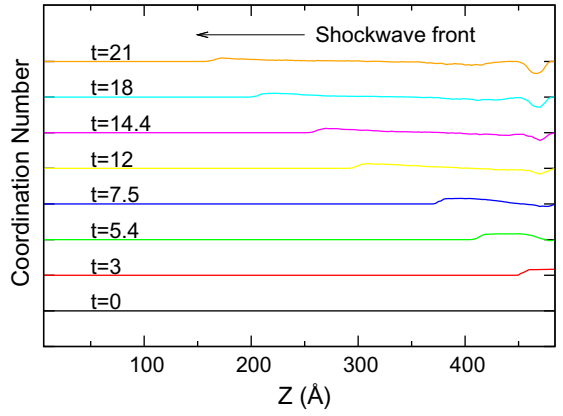

Fig. 8. Coordination number across the sample, at different times (see inset in ps). At the initial time $t = 0$, coordination number is 12. Curves at different times have been shifted for clarity. In the figure, the shockwave front is passing across the sample from right to left, as the arrow indicates.

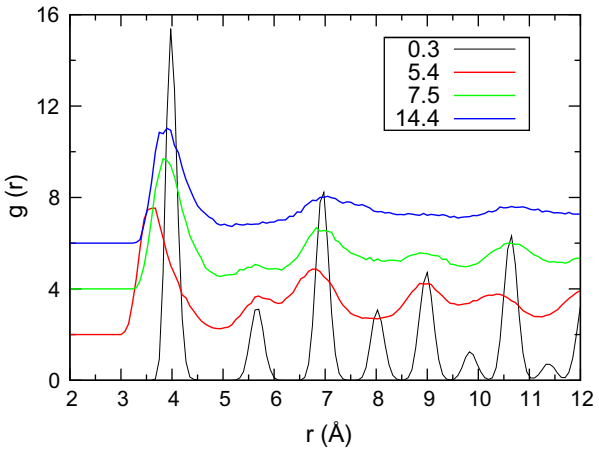

Fig. 9. Pair–distribution function calculated in the zone of failure, at four different times (see inset in ps). Curves at different times have been shifted for clarity.

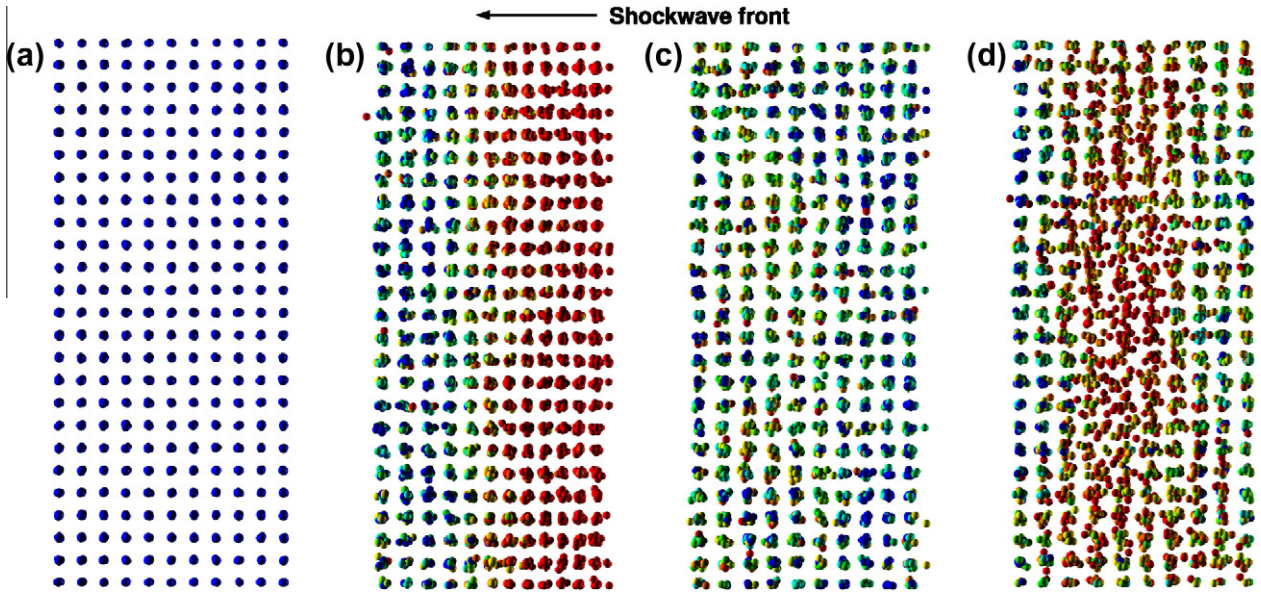

Fig. 10. Snapshots of the zone of failure, at four different times. The shockwave is passing across the sample from right to left, as the arrow indicates. Atoms are colored according to the CNA order parameter, from complete order (blue) to complete disorder (red). (a) $t = 0.3$ ps, before the shockwave reaches the region; (b) $t = 5.4$ ps, while the shockwave moves through the region; (c) $t = 7.5$ ps, after the shockwave passes, leaving some amount of structural disorder; and (d) $t = 14.4$ ps, the initiation of the failure process can be clearly seen from the accumulation of structural defects. (For interpretation of the references to color in this figure legend, the reader is referred to the web version of this article.)

that at the beginning there is a perfect fcc lattice (the straight line at $t = 0$), which become disordered according the shockwave advances (order parameter greater than zero). In Fig. 8 we show the coordination number. Initially, across the sample each atom has 12 nearest neighbors, and while the shockwave front advances through the sample the atoms increase their coordination number. But, in the zone where the material fails we can see, at $t = 7.5$ ps, that the coordination number begins to decrease below the initial value.

3.2. Failure of the material

Now we will describe in detail how the rupture of the sample is produced. This process has been described in different experimental and theoretical works [2,25], and is related to the spallation phenomenon. In this case, we are interested in studying, at an atomic level, what is the onset to this phenomenon and how it develops. For this, we will analyze in detail the rupture zone, which comprise the region between 453 Å and 484 Å, character-

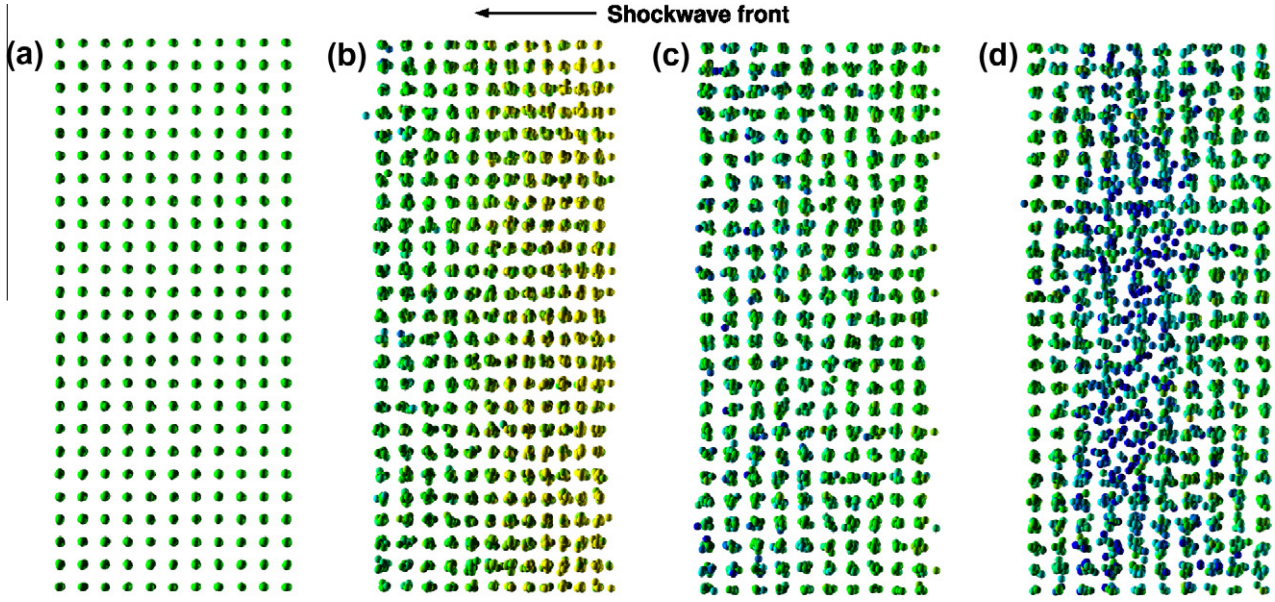

Fig. 11. Snapshots of the zone of failure, at four different times. The shockwave is passing across the sample from right to left, as the arrow indicates. Atoms are colored according to their coordination, where green atoms have the ideal coordination of the fcc lattice (12 nearest neighbors), blue atoms are undercoordinated and red atoms are overcoordinated. (a) $t = 0.3$ ps, before the shockwave reaches the region; (b) $t = 5.4$ ps while the shockwave moves through the region. The slightly yellow atoms indicate compression; (c) $t = 7.5$ ps, after the shockwave passes. Unlike Fig. 10, there is no remaining change in coordination; and (d) $t = 14.4$ ps, the formation of voids before the initiation of failure itself is manifest. (For interpretation of the references to color in this figure legend, the reader is referred to the web version of this article.)

ize their structure by evaluating the pair–distribution function, $g(r)$, in that region (Fig. 9) and through snapshots of the atoms colored according to the CNA order parameter (Fig. 10) and to the coordination number (Fig. 11), for different time steps.

The pair–distribution function is displayed in Fig. 9. Initially, at $t = 0.3$ ps, the sample is at 5 K and has a fcc structure (the width of the peaks is due to temperature effects). Then, the pair–distribution function displayed at $t = 5.4$ ps corresponds to the passage of the shockwave front across the rupture zone. At that moment, a high pressure and temperature develop, perturbating the initial crystalline structure. The $g(r)$ resemble the fcc structure, but the first peak indicate that the distance to the first neighbors is less than the initial value by 0.5 Å. This is consistent with the highly distorted fcc lattice shown in CNA order parameter and displayed in Fig. 7. At $t = 7.5$ ps, just after the passage of the shockwave front across the rupture zone, as it can be seen in Figs. 4–6, the pair–distribution function shows clearly that the first peak shifts to the right, but does not return to the initial value. Therefore, although the pressure has decreased in that zone, the structure is different, a liquid-like one. Finally, at $t = 14.4$ ps the second peak disappear, collapsing to the third peaks, a clear signature that the zone is in the liquid state. This condition remains in time until the zone fails.

This process can be better described by the snapshots shown in Figs. 10 and 11. They correspond to same times shown in Fig. 9, ranging from $t = 0.3$ ps the leftmost to $t = 14.4$ ps the rightmost. These figures show the atoms colored according to the CNA order parameter and the coordination number, respectively. The CNA order parameter color code goes from red (minimum percent of fcc order) to blue (maximum percent of fcc order) with the respective color gradation within it. For the coordination number, the color goes down from green (fcc coordination number, 12) to blue (minimum coordination number), and up to red (maximum coordination number) with the respective color gradation within it.

From left to right, Figs. 10 and 11 show initially a fcc structure, blue color for CNA order parameter and green color for the coordination number. Then at $t = 5.4$ ps in both analysis it can be seen that the shockwave front (red in CNA order parameter and yellow in coordination number) is passing through the selected area. At $t = 7.5$ ps, after the passage of the shockwave front, the atoms have different values from the initial ones, only a few retaining their original color. Finally, at $t = 14.4$ ps, a large number of atoms have lost completely their fcc order, as shown in CNA order parameter by the red color and the blue color in the coordination number. Also, the development of voids due to the rarefaction wave can be clearly seen. In this situation, defects play the role of nucleation centers for disorder, allowing some regions to reach the liquid state. Then, the vacancies coalesce, starting the formation and growth of cavities [25]. At the end, the material reaches the point where it is no longer able to withstand the tensile stress, causing the rupture.

4. Conclusion

In summary, we have simulated and analyzed the passage of a shockwave in solid argon by molecular dynamics. Our results indicate that the shockwave produced by the piston injects energy resulting in an increase of entropy, by way of heating the sample and producing a configurational disorder. On the front of the shockwave, a zone of high density, stress and temperature is generated, and its passage destroys the crystalline order of the material and creates defects such as vacancies. When the piston stops, a rarefaction wave is generated and moves backwards, causing low density zones. The vacancies coalesce, starting the formation and growth of cavities that later produce a decrease in the strength of the material and finally its failure.

Acknowledgments

This work has been supported by grant Anillo ACT/24-Chile "Computer simulation lab of nanobio system". PhD fellowships from Conicyt (CL) and Mecesup UCH008 (JP) are gratefully acknowledged.

References

[1] J.W. Martin, Concise Encyclopedia of Mechanical Properties of Materials, New York, 2007.
[2] A.K. Zurek, W.R. Thissell, J.N. Johnson, D.L. Tonks, R. Hixson, Journal of Materials Processing Technology 60 (1996) 261.
[3] D.L. Tonks, Journal de Physique IV 4 (1994) c8.
[4] M. Ortiz, A. Molinari, Journal of Applied Mechanics 59 (1999) 48.
[5] A.B. Belonoshko, Science 275 (1997) 955.
[6] Y.B. Zeldovich, Y.P. Raizer, Physics of Shock Waves and High-Temperature Hydrodynamic Phenomena, New York, 1966.
[7] L.D. Landau, E.M. Lifshitz, Fluid Mechanics, second ed., Amsterdam, 2004.
[8] B.L. Holian, G.K. Straub, Physical Review Letters 43 (1979) 1598.
[9] B.L. Holian, Shock Waves 5 (1995) 149.
[10] B.L. Holian, Physical Review A 37 (1988) 2562.
[11] B.L. Holian, P.S. Lomdahl, Science 280 (1998) 2085.
[12] E.M. Bringa, A. Caro, Y. Wang, M. Victoria, J.M. McNaney, B.A. Remington, R.F. Smith, B.R. Torralva, H.V. Swygenhoven, Science 309 (2005) 1838.
[13] D. Tanguy, M. Mareschal, T.C. Germann, B.L. Holian, P.S. Lomdahl, R. Ravelo, Materials Science and Engineering A 387 (2004) 262.
[14] P.S. Branicio, R.K. Kalia, A. Nakano, P. Vashishta, F. Shimojo, J.P. Rino, Journal of the Mechanics and Physics of Solids 56 (2008) 1955.
[15] S. Stishov, I. Makarenko, V. Ivanov, V. Pedoslmov, Journal of Experimental and Theoretical Physics Letter 11 (1970) 13.
[16] M. Ross, H.K. Mao, P.M. Bell, J.A. Xu, Journal of Chemical Physics 85 (1986) 1028.
[17] A. Jayaraman, Review of Scientific Instruments 57 (1986) 1013.
[18] The simulations were done using an in-house code, Las Palmeras Molecular Dynamics, <www.gnm.cl/lpmd>.
[19] M. Ross, Physical Review A 8 (1973) 1466.
[20] R.D. Dick, R.H. Warnes, J. Skalyo, The Journal of Chemical Physics 53 (1970) 1648.
[21] H. Meixner, P. Leiderer, E. Luscher, Physics Letters A 37 (1971) 39.
[22] B.L. Holian, W.G. Hoover, B. Moran, G.K. Straub, Physical Review A 22 (1980) 2798.
[23] J.D. Honeycutt, H.C. Andersen, The Journal of Physical Chemistry 91 (1987) 4950.
[24] K. Sokolowki-Tinten, J. Bialkowski, A. Cavalleri, D. von der Linde, A. Oparin, J. Meyer-ter-Vehn, S.I. Anisimov, Physical Review Letters 81 (1998) 224.
[25] A. Strachan, T. Cagin, W.A. Goddard, Physical Review B 63 (2001) 060103(R).